Government of **Western Australia**
Department of **Mines and Petroleum**

RECORD 2013/12

THE IRONSTONE VEINS OF THE GIFFORD CREEK FERROCARBONATITE COMPLEX, GASCOYNE PROVINCE

by
F Pirajno and I González-Álvarez

Geological Survey of Western Australia

Government of **Western Australia**
Department of **Mines and Petroleum**

Record 2013/12

THE IRONSTONE VEINS OF THE GIFFORD CREEK FERROCARBONATITE COMPLEX, GASCOYNE PROVINCE

by
F Pirajno and I González-Álvarez

Perth 2013

Geological Survey of Western Australia

MINISTER FOR MINES AND PETROLEUM
Hon. Bill Marmion MLA

DIRECTOR GENERAL, DEPARTMENT OF MINES AND PETROLEUM
Richard Sellers

EXECUTIVE DIRECTOR, GEOLOGICAL SURVEY OF WESTERN AUSTRALIA
Rick Rogerson

REFERENCE
The recommended reference for this publication is:
Pirajno, F and González-Álvarez, I 2013, The ironstone veins of the Gifford Creek ferrocarbonatite complex, Gascoyne Province: Geological Survey of Western Australia, Record 2013/12, 19p.

National Library of Australia Card Number and ISBN PDF 978-1-74168-524-4

Grid references in this publication refer to the Geocentric Datum of Australia 1994 (GDA94). Locations mentioned in the text are referenced using Map Grid Australia (MGA) coordinates, Zone 50. All locations are quoted to at least the nearest 100 m.

Published 2013 by Geological Survey of Western Australia
This Record is published in digital format (PDF) and is available online at <www.dmp.wa.gov.au/GSWApublications>.

Further details of geological products and maps produced by the Geological Survey of Western Australia are available from:
Information Centre
Department of Mines and Petroleum
100 Plain Street
EAST PERTH WESTERN AUSTRALIA 6004
Telephone: +61 8 9222 3459   Facsimile: +61 8 9222 3444
www.dmp.wa.gov.au/GSWApublications

Contents

Figures

Table

The ironstone veins of the Gifford Creek Ferrocarbonatite Complex, Gascoyne Province

by

Franco Pirajno and Ignacio González-Álvarez[1]

Abstract

The Gifford Creek Ferrocarbonatite Complex comprises sills, dykes, and veins of ferrocarbonatite, intruding the Pimbyana Granite and Yangibana Granite of the Durlacher Supersuite and metasedimentary rocks of the Pooranoo Metamorphics in the Gascoyne Province.

The ferrocarbonatite intrusions have a general northwesterly trend, parallel with and adjacent to the Lyons River Fault. To the north of the Lyons River Fault, arcuate and sinuous veins of iron oxides (magnetite, hematite and goethite), referred to as ironstones, are distributed within a ca. 25 x 25 km zone, locally associated with quartz veins that were likely formed during post-magmatic alteration processes. Closer inspection of these ironstone veins shows that they have relic ferrocarbonatite margins, associated with wallrocks of fenitic character. These veins were formed from various alteration stages of the iron carbonates that dominate the original carbonatite material. The fenitic haloes are characterized by the presence of feldspars and/or Na-amphiboles and magnetite, as well as economically important minerals such as monazite, pyrochlore, and columbite–tantalite group minerals.

Most mineral exploration in the area has focused on these ironstone veins, due to their gossan-like 'high-visibility'. The ironstone veins were first explored by mining companies for their rare earth element potential. Subsequently, the ferrocarbonatites and the ironstone veins were the subject of a PhD project (Pearson, 1996). More recently and continuing today are exploration efforts conducted by the private sector to reassess the rare earth mineral potential of the ironstone veins, in the light of current favourable economic trends.

This Record integrates previous (published and unpublished) work on the nature of the ironstone veins and their wallrocks with new field observations, and analytical and petrological data, to develop a model that attempts to explain the evolutionary stages of the ironstone veins from the original ferrocarbonatite.

KEYWORDS: alteration, exploration, iron oxides, magmatic deposits, magmatism, metasediments, mineralization, petrology, rare earth elements

Introduction and geological setting

The Gifford Creek Ferrocarbonatite Complex lies within the Gascoyne Province, which is located between the Archean Yilgarn Craton and the Pilbara Craton. The Province is overlain to the north by the Paleoproterozoic Ashburton Formation, the Mesoproterozoic Edmund and Collier Basins to the east, and the Phanerozoic Carnarvon Basin to the west (Fig. 1). The Province consists of a suite of Neoarchean to Paleoproterozoic granite gneisses and metasedimentary rocks (Johnson et al., 2011a,b). These are interpreted as basement to various Proterozoic rocks, including granitic rocks of the 1680–1620 Ma Durlacher Supersuite and metasedimentary successions of the 1760–1680 Pooranoo Metamorphics. Details of the geology of the Province are provided by Martin et al. (2006), Sheppard et al. (2007, 2010), Johnson et al. (2011a,b,c), and an overview of its mineralization by Flint and Abeysinghe (2000). In the Gascoyne Province, at least five tectono-thermal events have been recognized (with a possible sixth also listed):

1. 2005–1950 Ma Glenburgh Orogeny (Johnson et al., 2011b)
2. 1820–1770 Ma Capricorn Orogeny (Sheppard et al., 2011)
3. 1680–1620 Ma Mangaroon Orogeny (Sheppard et al., 2007)
4. 1385–1170 Ma Mutherbukin Tectonic Event (Johnson et al., 2009)
5. 1030–955 Ma Edmundian Orogeny (Sheppard et al., 2007)

1 CSIRO, Australian Resources Research Centre, Minerals Down Under National Flagship, Discovery Theme, Kensington WA 6151

6. A possible Neoproterozoic event at ca. 570 Ma Mulka Tectonic Event (Sheppard et al., 2010). The Gascoyne Province was later intruded by the 755 Ma Mundine Well Dolerite Suite (Wingate and Giddings, 2000), and then cut by east-southeast-trending shear zones at 570 Ma (Mulka event; Sheppard et al., 2010).

Pearson (1996), Pearson et al. (1996) and Pearson and Taylor (1996) first studied altered rocks, dykes of alkaline composition and associated ironstone veins, intruding the Proterozoic granitic rocks of the Gascoyne Province. They recognized high-level alkaline intrusions within a 1.6 – 1.8 Ga granitic basement. Two alkaline magmatic episodes were described:

1. A swarm of ultrabasic intrusions emplaced prior to the deposition of the Bangemall Supergroup at c. 1680 Ma

2. A younger phase of dykes and sills of carbonatitic affinity that intrude the Bangemall Supergroup.

They named these alkaline rocks, the Gifford Creek Igneous Complex.

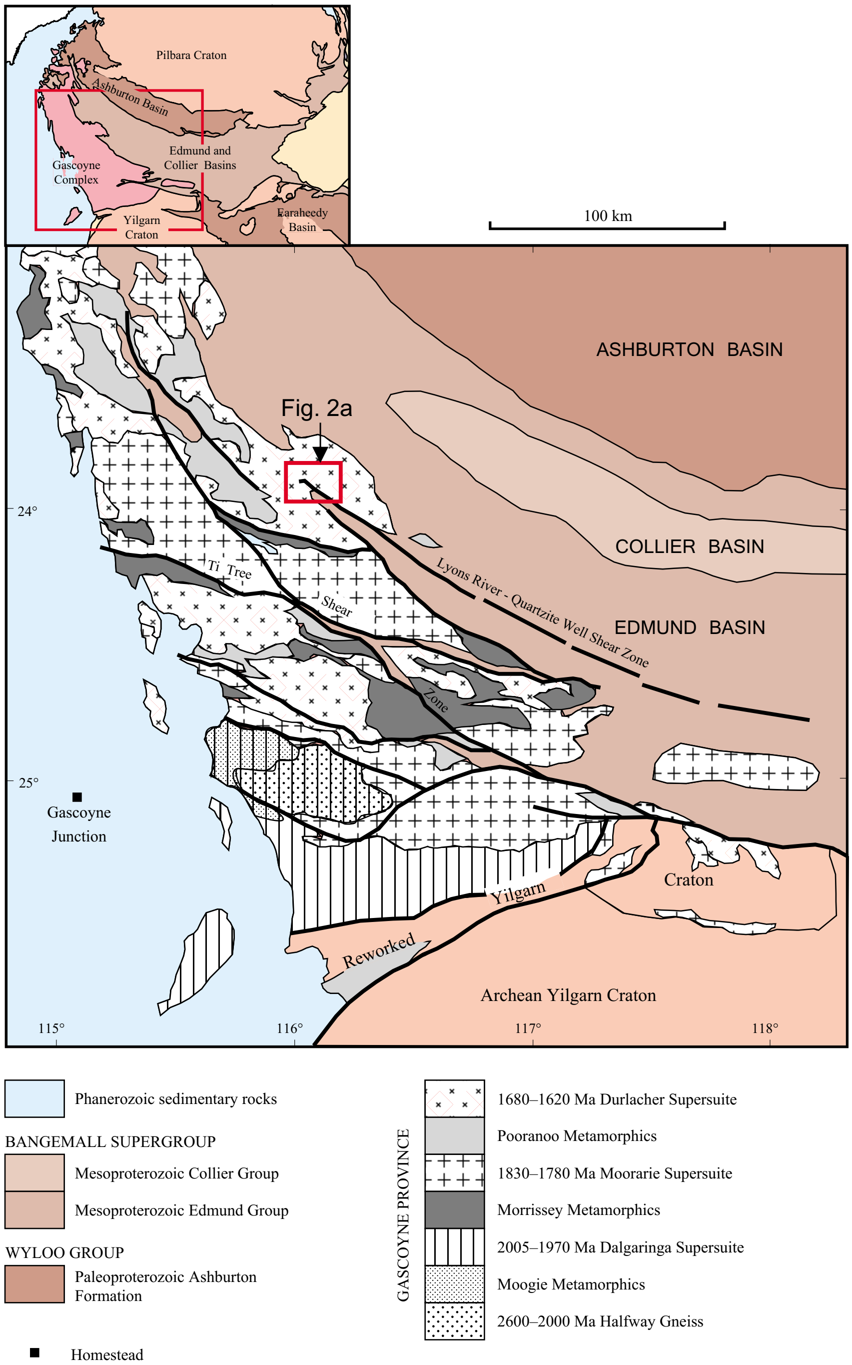

Figure 1. Regional geological setting of the Gascoyne Province (modified after Sheppard et al., 2010), showing location of the area of Figure 2

On the basis of Pearson and co-authors' work and our own studies, we recognized the Gifford Creek Complex to be a carbonatite complex (rocks with >50% carbonates, fluoroapatite, nepheline and other feldspathoids), characterized by ferrocarbonatite dykes, veins and sills, that are surrounded by variably fenitized country rocks. Hence, it was renamed the Gifford Creek Carbonatite Complex (Pirajno et al., 2010). However, due to the preponderance of iron carbonate, in some cases exclusively, the name of Gifford Creek Ferrocarbonatite Complex (thereafter referred to as GFC) is considered more appropriate. The Gifford Creek rocks have also been considered as a Suite, rather than a Complex (Johnson, 2013). However, we prefer to retain the term Complex, because the Gifford Creek lithologies show irregular and complex structural and compositional features unlike, for example, a dolerite suite.

This study focused on one of the main features of the GFC, namely the widespread occurrence of ironstone (mainly magnetite, hematite and goethite) veins that are spatially associated with the ferrocarbonatite intrusions and are surrounded by relatively narrow haloes of fenitic alteration. The term ironstone, defined by Neuendorf et al. (2005), as 'any rock containing a substantial proportion of an iron compound', can be applied to the Gifford iron oxide veins, but the term ironstone used in this study specifically refers to massive, or near massive, iron oxides. These veins of iron oxides are also locally associated with quartz veins, interpreted to have formed during post-magmatic alteration processes. Further work is underway to address the nature and age of the ferrocarbonatite intrusions.

Detailed studies on the ironstone veins, including the use of scanning electron microscopy (SEM), X-ray diffraction (XRD) and petrographic studies, integrated with field observations, has led us to propose a new model to explain the origin of the ironstone.

Regional overview of the Gifford Creek Ferrocarbonatite Complex

Pearson (1996), Pearson and Taylor (1996) and Pearson et al. (1996) reported on the nature, petrography and mineral chemistry of various rocks from the complex, which they called Lyons River ultrabasic sills. These scientists recognized extensive fenitization of the granitic country rocks of the Paleoproterozoic Gascoyne Province (Sheppard et al., 2010), associated with the abovementioned ironstone veins. Pearson et al. (1996) also pointed out that the GFC represents the largest complex of its kind in Australia, occupying an area of about 700 km^2 (Fig. 2). Pearson and her co-authors recognized that the Lyons River sills consist of primary-textured ultrabasic rocks, which they classified as blue sills, light-brown sills, dark-brown sills and green sills. Apart from the colour, these rocks contain variable proportions of sodic amphibole, sodic pyroxene, apatite, barite, monazite, phlogopite and Fe–Ti oxides. An important aspect is that many, if not all, contain more than 50% by volume of iron-rich carbonate material (dolomite, ankerite) and lesser calcite, which places the nomenclature of these rocks in the carbonatite field (Le Maitre, 2002) and more specifically ferrocarbonatite. Detailed mapping shows that the ferrocarbonatite sills and dykes form a northwest-trending belt in the southwestern sector of the GFC (Fig. 2), parallel to, and adjacent to the north side of the Lyons River Fault.

The age of the GFC is unknown, but field relationships indicate that it must be younger than the 1675–1773 Ma Pimbyana Granite and the 1660–1659 Ma Yangibana Granite. These ferrocarbonatites could have been emplaced during the thermal reworking of the Capricorn Orogen, which may have occurred during the emplacement of the c. 1075 Ma Warakurna large igneous province, or the c. 755 Ma Mundine Dolerite Suite (Wingate et al., 2004; Wingate and Giddings, 2000; Sheppard et al., 2007; 2010). We assume that the ironstone veins are coeval with the ferrocarbonatite intrusions, but this awaits confirmation by in situ U–Pb dating of apatite by LA–ICP–MS, which is in progress. We plan to present those results in a separate contribution.

Flint and Abeysinghe (2000) recorded rare earth elements (REE) and uranium mineralization in the ferrocarbonatite and ironstone veins and quoted pre-JORC 1989 estimated combined resources of 3.5 Mt, averaging 1.7% REE oxides. Recent drilling by Hasting Rare Metals Ltd at Yangibana reported low grades of the heavy rare earth oxides (HREO), but of particular interest is the high neodymium grade which averages around 4000 ppm Nd_2O_3, or 24% of the total rare earth oxides (TREO) (Hastings Rare Metals Ltd, 2012).

To the north of the Lyons River Fault, numerous sinuous ironstone veins and pods (Fig. 2), the focus of this Record, are enclosed or surrounded by zones of fenitization of the country rocks (Pimbyana Granite and other granitic units of the 1680–1620 Ma Durlacher Supersuite (Sheppard et al., 2007, 2010). The ironstone veins, with dominant north, northeast and west-northwest trends (Fig. 2), consist of magnetite, hematite and supergene goethite and are locally radioactive (measured with a scintillometre cps of +1000). Exploration drilling indicated that some of these ironstones can be traced at depth to narrow (5–10 m thick) ferrocarbonatite dykes (Newcrest Mining Ltd, 1991). This was also recognized by Pearson et al. (1996) and confirmed by our field observations, whereby the ferrocarbonatite sill-like and dyke intrusions locally exhibit a gradual transition to iron oxides.

Analytical methods

X-ray diffraction (XRD) analyses

Samples of the ironstone veins and their fenitic haloes were examined using petrographic, energy dispersive X-ray analysis (EDX), X-ray powder diffraction (XRPD) and scanning electron microprobe (SEM) techniques. Due to the difficulty of identifying unusual mineral species by conventional optical microscopy, a suite of six polished

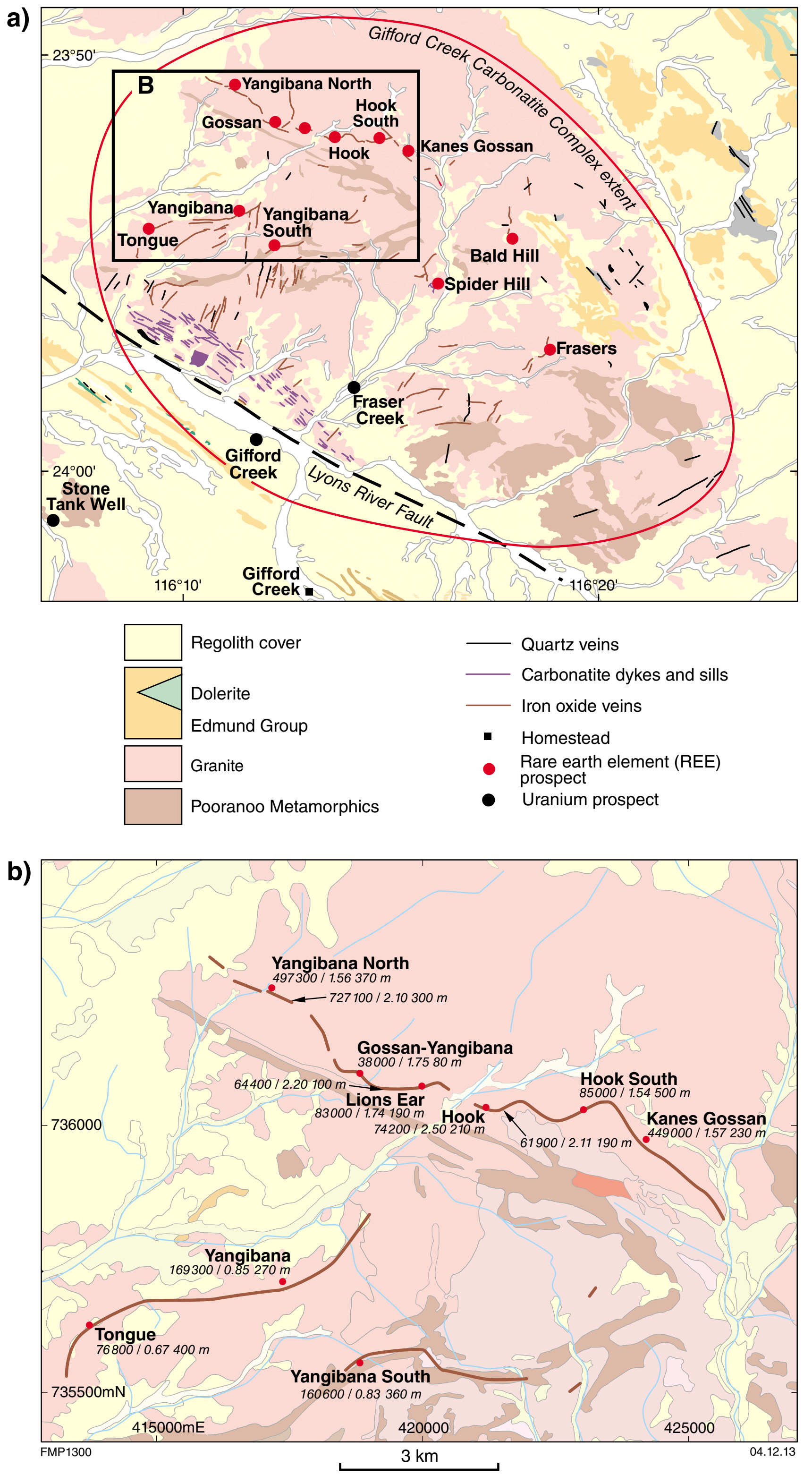

Figure 2. a) Simplified geological map of Gifford Creek Ferrocarbonatite Complex, showing ironstone veins, dykes and northwest-trending belt of ferrocarbonatite dykes and sills (formerly called Lyons River ultrabasic sills; Pearson et al., 1996). Also shown are the main REE prospects investigated by drilling; b) Sketch map showing distribution of the prospects, with defined non-JORC compliant resources (1988) (tonnes/% TREO length in metres) within current tenements owned by Hastings Rare Metals Ltd. Image courtesy of Andy Border of Hastings Rare Metals Ltd.

thin sections was selected for EDX, XRPD and SEM analyses. Results of XRPD analyses are presented in Table 1.

Back-scattered (BSE) and secondary electron (SE) images on a set of two samples are shown in Figures 3 to 5. These samples showed minimal weathering (GSWA 197996, GSWA 197986).

All samples were initially examined under a stereoscopic light microscope before representative subsets of the rock were used for XRPD analysis, in order to detect individual mineral species. The methodology used is summarized below.

For XRPD, rock thin section offcuts were examined using a stereoscopic microscope and subsamples obtained by abrading the surface with a tungsten carbide pencil. Resulting powders were further pulverized and mounted on quartz plates for XRPD. For EDX, the chemical composition of mineral grains was determined by examination of carbon-coated polished thin sections using an SEM (CamScan CS3200 LV) connected to an EDX (Oxford INCA).

Scanning electron microscope (SEM) analyses

Follow-up SEM was carried out on the cited six polished thin sections using a Jeol JSM–6400 SEM (housed at the Centre for Microscopy, Characterisation and Analysis at The University of Western Australia), and configured with Link ISIS energy dispersive system (EDS).

Mineral identifications were checked and confirmed by semiquantitative EDS. Calibration of the EDS for quantitative analysis was performed on pure Cu for standard conditions for silicates and oxides. Operating conditions used were an accelerating voltage of 15 kV and a beam current of 5nA.

The SEM was used to characterize the mineral morphology and composition in the sample suite. Mineral identification was facilitated using XPLOT search-match software (www.ccp14.ac.uk/solution/search-match.htm).

Results

Petrography of selected samples

Samples GSWA 197996, 197986, 197987 and 186707 were first examined by conventional optical microscopy, followed by SEM analysis. Brief descriptions follow.

GSWA 197996 is a fenite with a mineralogical association of K-feldspar (sanidine and K–Na feldspar), sodic pyroxene (aegirine–augite), quartz, alkali amphibole(?), and accessory amounts of monazite, barite, celestite, and zircon. Minerals show an intensive alteration by iron oxides and element exsolution in the K–Na–Ca feldspar series and sodic pyroxenes (aegirine–augite). Abundant heavy mineral inclusions in feldspars and pyroxenes of <15 µm size comprise monazite, zircon, barite and celestite (Fig. 3).

GSWA 197986 is an ironstone composed of magnetite, barite and monazite in a matrix of iron oxide. The magnetite occurs as large phenocrysts up to 1 mm. Fractions of <15 µm comprise euhedral barite and rounded monazite grains disseminated in a matrix of iron oxides (Fig. 4). All mineral phases are severely affected by iron oxide alteration.

GSWA 197987 is an ironstone, that contains abundant barite and rounded monazite grains disseminated in a matrix of largely amorphous iron oxide (with some traces of mica) rich in Na and P (Fig. 5). The barite grains are commonly larger than 100 µm and with a skeletal texture, reflecting severe oxidation of the original barite grains. All mineral phases are affected by varying degrees of iron oxide alteration. The textural features of the carbonatite protolith have been obliterated leaving an insoluble fraction of bastnaesite, pyrochlore, ferrocolumbite, and monazite.

Table 1. Results of XRPD diffraction analyses; concentration of crystalline phases estimated from peak intensity: dominant = > 40%; major = 10–40%; minor = 2–10%; trace = 2%; nd = not detected

GSWA sample no.	*Quartz*	*Microcline*	*Plagioclase*	*Ferromagnesian mica*	*Na-amphibole*	*Aegirine*	*Calcite*	*Dolomite*
197991	nd	nd	nd	nd	major	trace	major	major
197992	nd	nd	nd	nd	nd	major	nd	dominant
197994	major	major	major	minor	nd	nd	nd	nd
197998	trace	dominant	nd	major	nd	nd	nd	nd

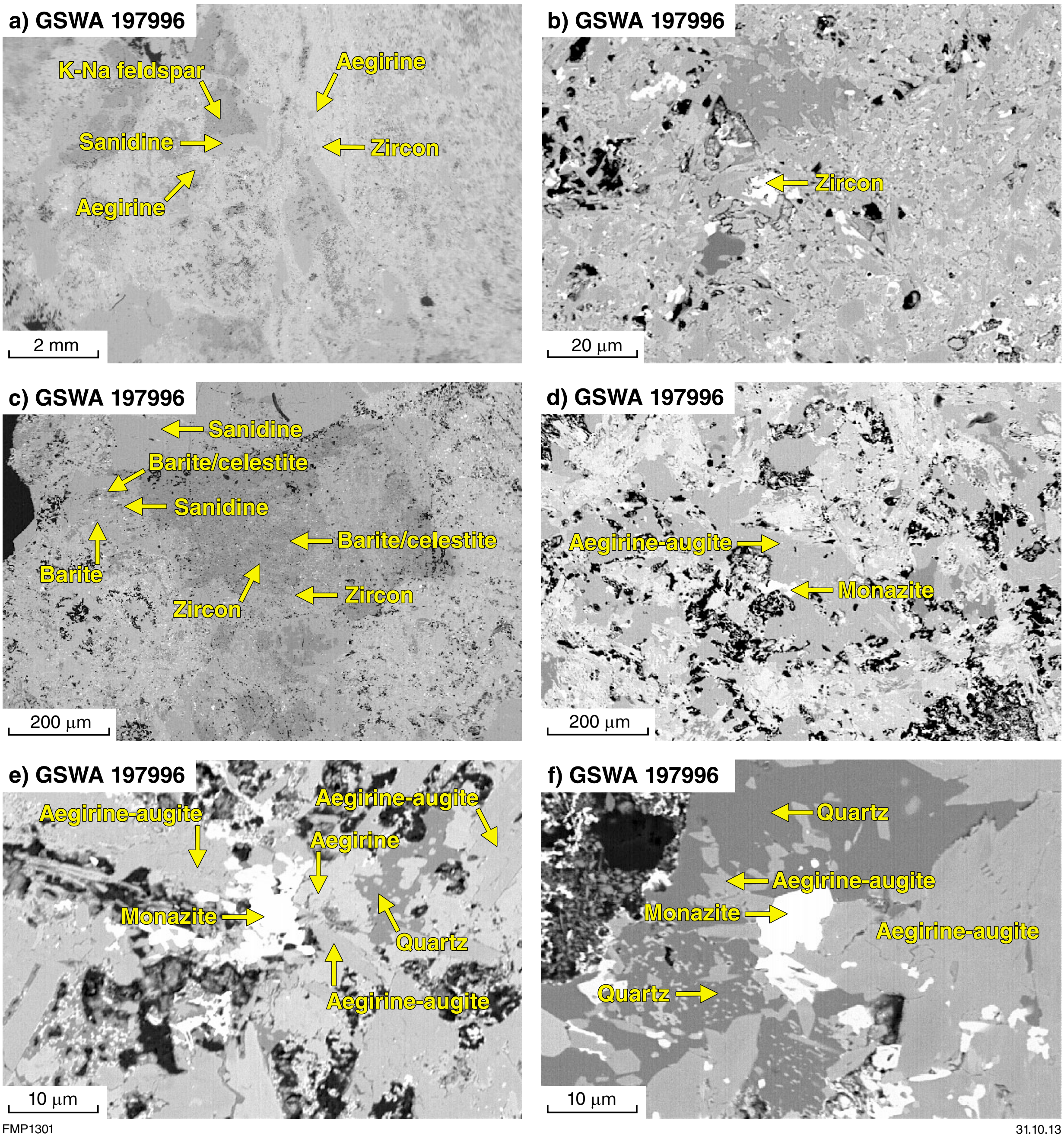

Figure 3. Backscattered electron photomicrographs of a fenitic rock (sample GSWA 197996), illustrating some of the textures and distribution of aegirine, sanidine, apatite and zircon (a and b), barite and celestite (c), monazite and aegirine–augite (d, e and f)

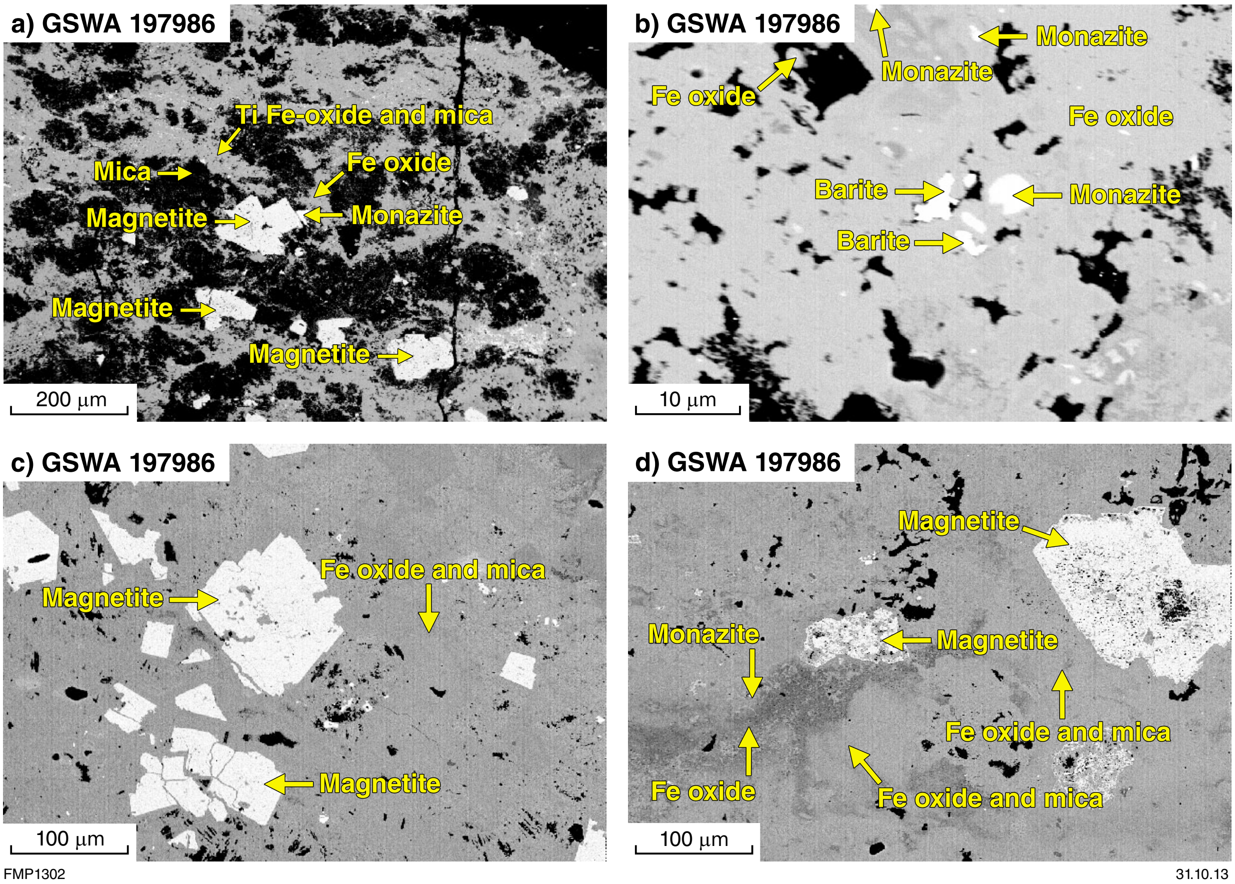

Figure 4. Backscattered electron photomicrographs of sample GSWA 197986: a), c) and d) display phenocrysts of magnetite within an iron oxide – mica matrix; b) shows abundant heavy mineral content in monazite and barite; d) displays intense alteration of magnetite phenocrysts

GSWA 186707 is from a 15 cm-thick iron oxide vein flanked by fenitic alteration cutting through a megacrystic granite of the Durlacher Supersuite (Fig. 6a). The fenitic halo consists of a phlogopite ± quartz assemblage, with irregular zones of acicular riebeckite, overprinted by iron oxides (hematite and magnetite), locally reaching a massive texture. SEM analyses of this sample showed monazite, ferrocolumbite, a single grain of galena and an unidentified Ce–La oxide.

Previously described mineral chemistry

Pearson et al. (1996) investigated the mineral chemistry of the more common phases of carbonatites and fenitic rocks of the GFC. Alkali amphibole has compositions ranging from potassian magnesio-arfvedsonite to magnesio-riebeckite. The amphiboles in the fenitic rocks are classified as potassium magnesio-fluor-arfvedsonite ($KNa_2Mg_4Fe^{3+}Si_8O_{22}F_2$). Sodic pyroxene is generally aegirine with a high $Na(Fe_{3+}Si_2)_6$ component with TiO_2 contents of up to 4 wt%. Mica is metasomatic and Al-deficient presented as fluorophlogopite (fluorine contents from 1.5 to 4.5 wt%). Apatite is characterized by zoned crystals with fluorine contents of between 3 and 4 wt% and Ce_2O_3 ranging from 0.1 to 0.5 wt%.

Pearson et al. (1996) pointed out that the GFC micas are compositionally similar to the micas (phlogopite) of kimberlite and ultramafic lamprophyres, and reported complex zoned ferroan dolomite and ferroan magnesite, as the main carbonate phases.

Gifford Creek ironstones and wallrock fenites

The ironstones

The GFC ironstone veins have sinuous or arcuate trends; locally they occur as pods of massive iron oxides and are generally between a few centimetres to about 10 m thick (Figs 6a, 7 and 8). Veins of hematite–magnetite, in places with supergene alteration to massive goethite, are locally associated with quartz veins (Fig. 2). The presence of

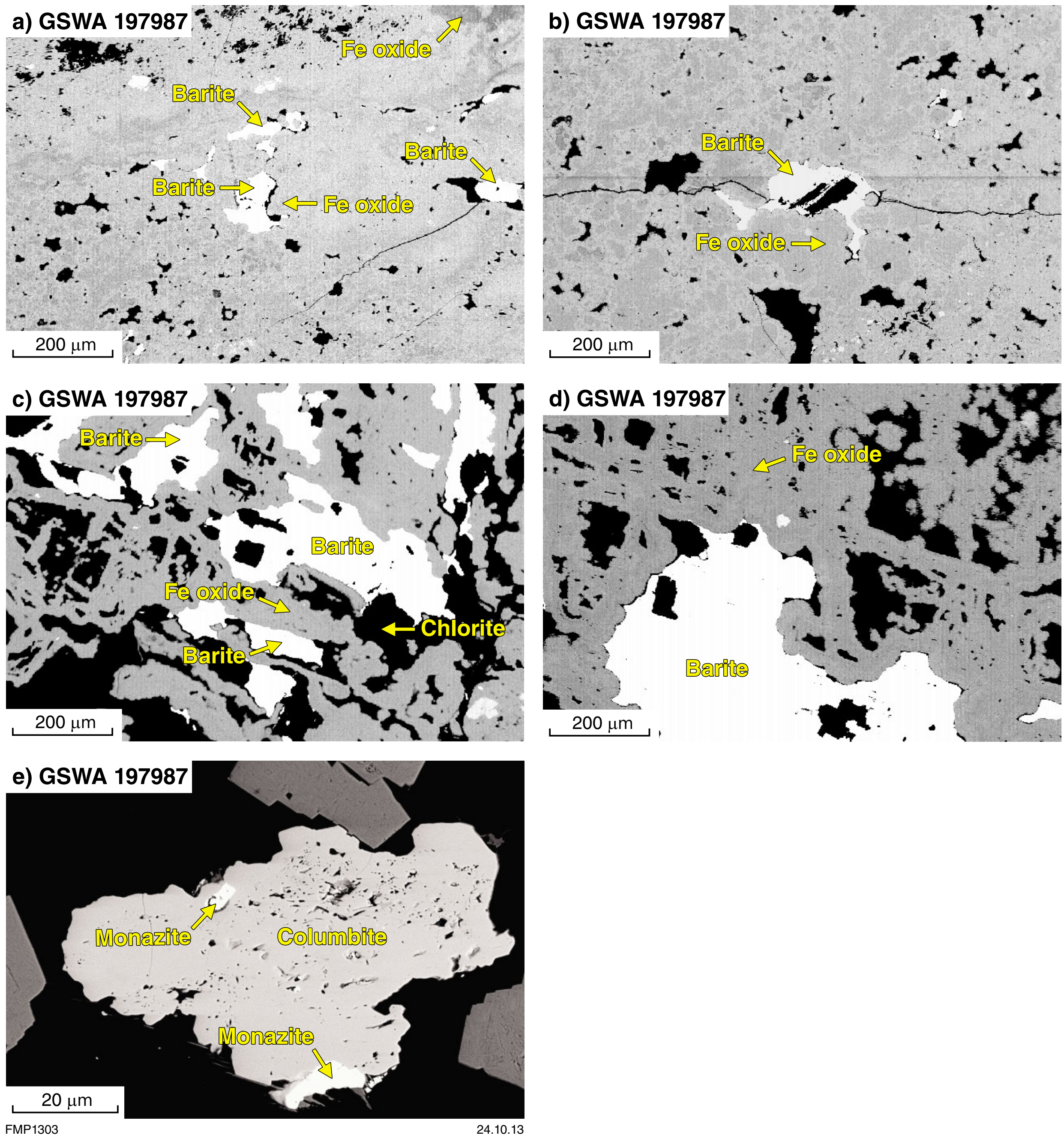

Figure 5. Backscattered electron photomicrographs of GSWA 197987. Images a) to d) reveal significant iron oxidation and large skeletal grains of barite; a grain of columbite with monazite is shown in e).

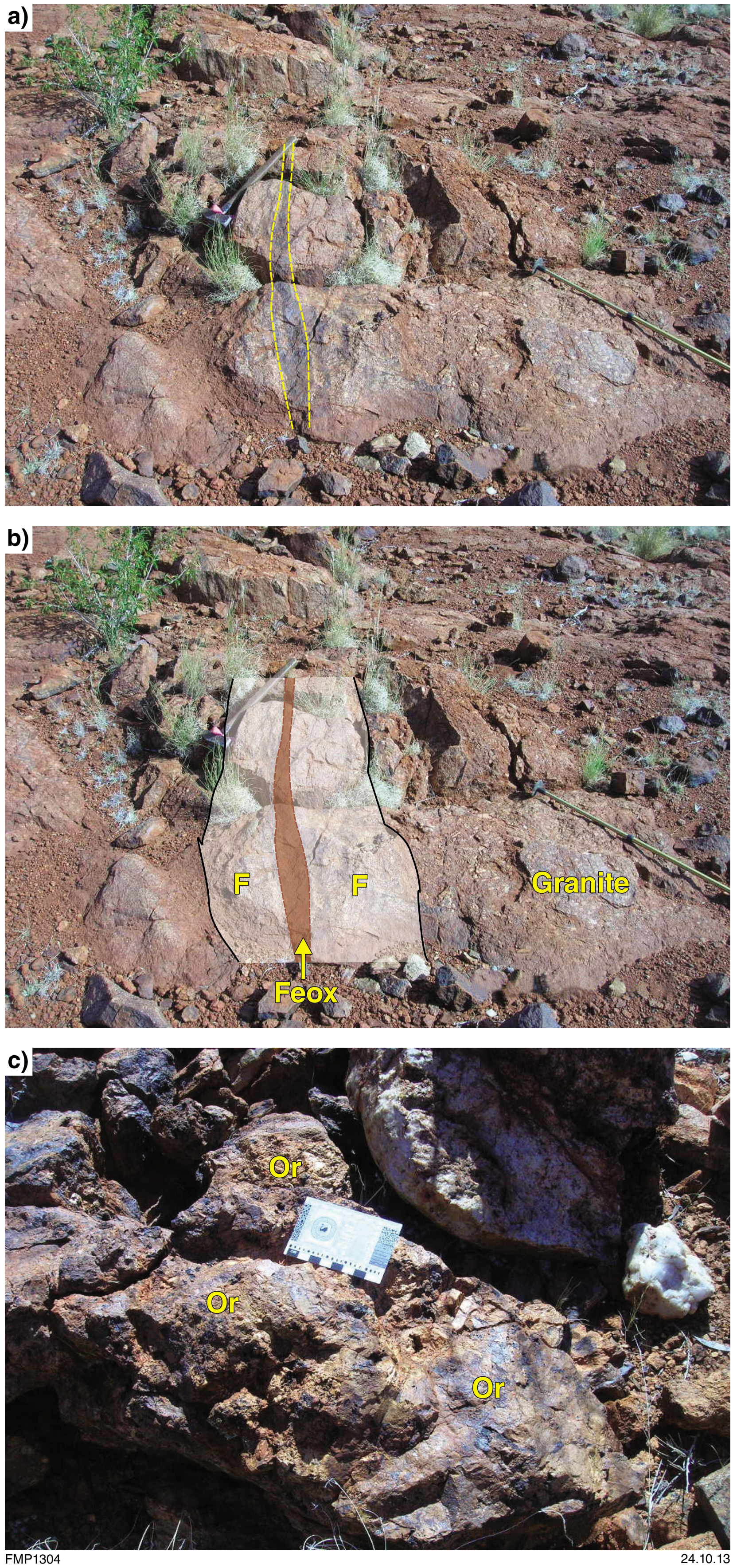

Figure 6. **a) and b) Outcrop showing a vein of fenitic alteration (F) and iron oxides (Feox) cutting a fenitized granite outcrop (sample GSWA 186707 was taken from this outcrop); c) orthoclasite rock (Or means orthoclase)**

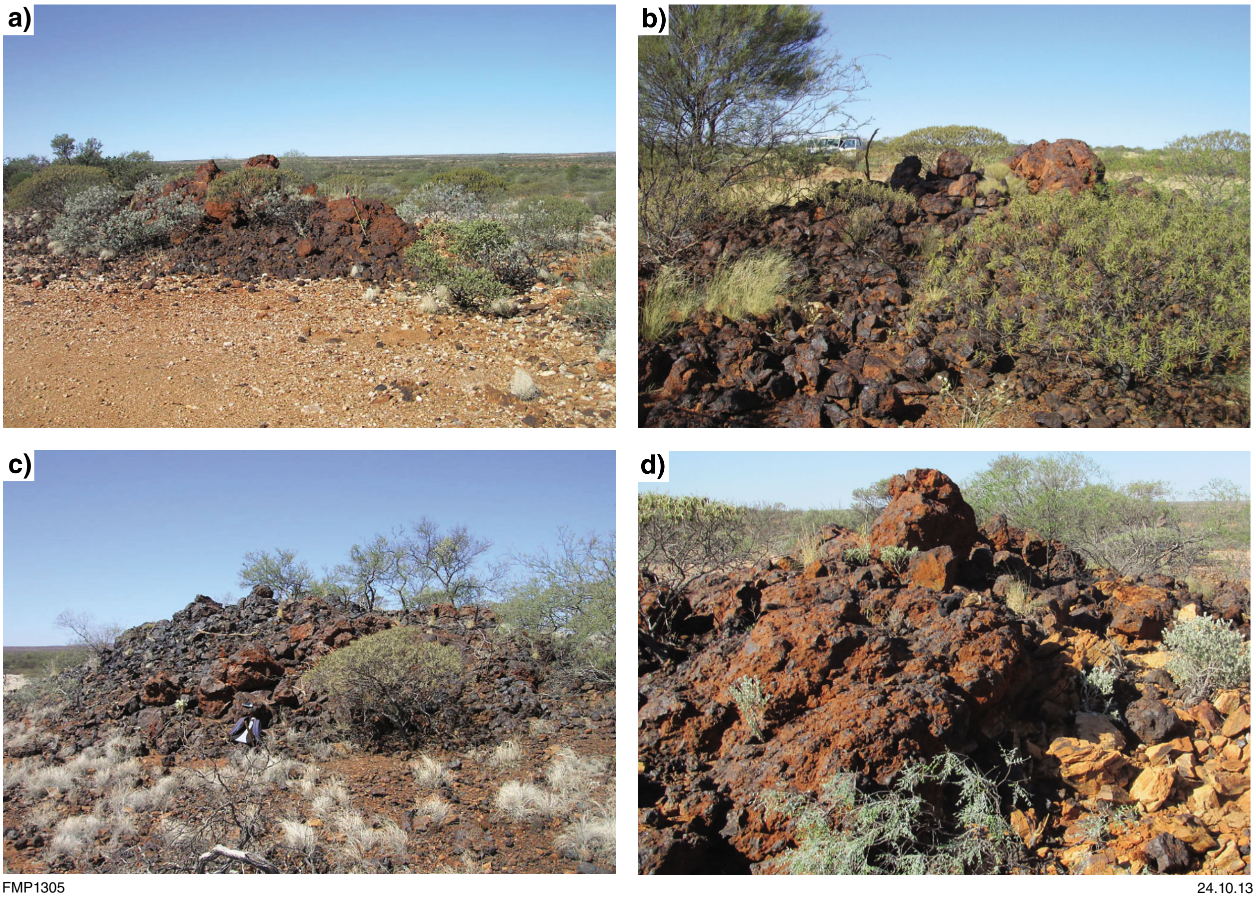

Figure 7. Typical outcrops of ironstone veins: a) Yangibana prospect; b) unnamed location (418658E 7355369N); c) unnamed location (425019E 7359093N); d) Tongue prospect; see Figure 2

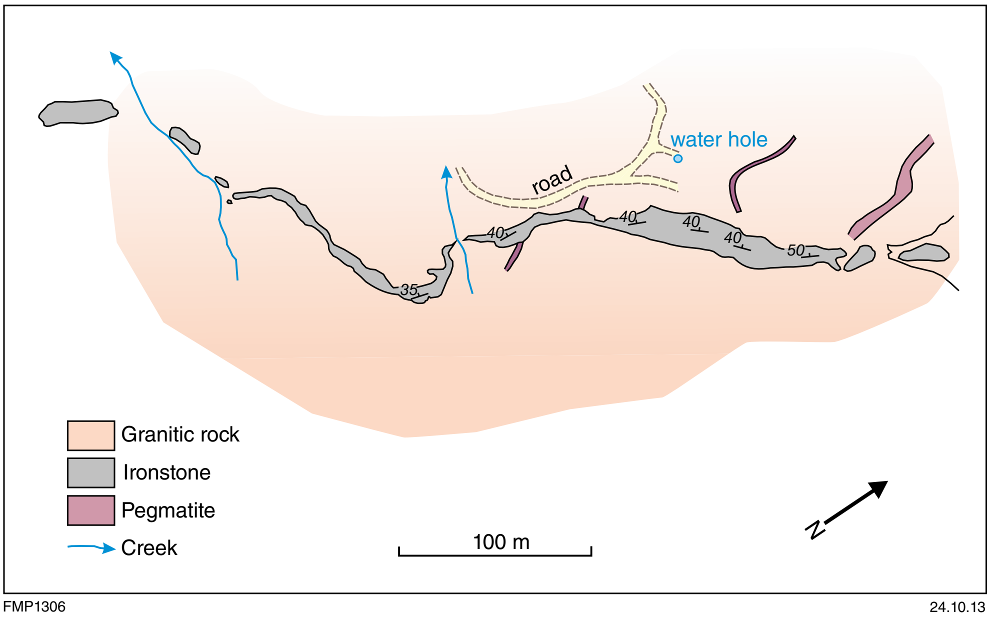

Figure 8. Plan view of the ironstone vein at Frasers prospect; after Pooley (1989) (no coordinates shown in the original report; refer to Figure 2a for approximate position)

quartz or calcite is attributed to later hydrothermal activity, distinct from the effects of iron oxide rich and fenitizing fluids. Attitude, field relationships, and petrographic data suggest that the ironstone veins postdate the emplacement of the ferrocarbonatite intrusions. Exploration reverse circulation (RC) drilling has shown that these veins have very shallow (c. 10°) to steep (c. 65°) dips (Fig. 8) (Pooley, 1988). The ironstone veins are arcuate to sinuous and have variable trends (Fig. 9), although in many instances they tend to be almost perpendicular to the trend of the ferrocarbonatites swarm of sills and dykes that run subparallel to the Lyons River Fault, on the southern margin of the GFC (Fig. 2). Pearson et al. (1996) reported the presence of magnetite pods (which are part of the ironstones) grading into narrow, flat-lying aegirine–apatite–phlogopite–magnetite–pyrochlore sheets. As shown in Fig. 2, some of the ironstones have been investigated for their REE and uranium mineral potential in a number of localities, such as Yangibana North and South, Yangibana, Spider Hill, Fraser, Lion's Ear, Hook and Hook South (see Fig. 9), Kane's Gossan and Tongue. These were investigated by field mapping and shallow drilling by exploration concerns in the 1970s and 1980s (Gellatly, 1975; Pearson et al., 1995; Pearson, 1996; Hoatson et al., 2011; see also Fig. 2). Renewed interest, particularly in theYangibana prospect is linked to their rare earth, uranium and thorium potential.

Diamond drillholes show that the ironstones grade at depth (Fig. 10) to ferrocarbonatite rocks, which are mainly constituted by iron carbonates (dolomite and ankerite), with subordinate amounts of magnetite, ferroan phlogopite, apatite, allanite, pyrite, sodic amphibole and aegirine. Monazite, pyrochlore, bastanesite, melilite, cancrinite, and lamprophyllite are present as accessory minerals. Traces of fluorite, sphalerite, molybdenite and galena were reported by Pearson et al. (1995).

The Tongue ironstone veins extend for about 400 m with thicknesses of 0.5 to 2.5 m (Pooley, 1988). This ironstone material is associated with fenitized rocks at the footwall, typically showing a cataclastic to fluidized texture, with cloudy feldspars (albite and orthoclase?) within a crushed matrix, and with iron oxides along grain boundaries and in crosscutting fractures.

The Yangibana ironstone is composed of massive and generally amorphous iron oxides with patches of relic or second-generation quartz (related to oxidation/weathering). In reflected light microscopy the iron oxides show at least three generations, from earliest to latest:

1. magnetite
2. hematite replacing pre-existing magnetite crystals (e.g. cubic) along crystallographic lines
3. dull, goethitic (oxyhydroxide) material.

The magnetite is rimmed by hematite. Colloform hematite and goethite, more or less banded, locally associated with bright yellow (carnotite?) patches and rims around the iron oxides. Crude banding is present, which may be related to the original ferrocarbonatite texture, or it may have developed during oxidation and regolith development. Magnetite is euhedral and probably is a primary mineral phase. It is spatially associated with bastnaesite, sodic amphibole or cancrinite, which form the matrix between the magnetite crystals. Thus, magnetite – bastnaesite – sodic amphibole – cancrinite is assumed to be part of a carbonatite system. Hematite on the other hand, appears to pervasively occupy fractures and cleavage traces, and may locally replace the main ferrocarbonatite or fenitic mineral assemblages. In this case and based on textural relationships, a possible paragenetic sequence is bastanaesite → sodic amphibole+cancrinite → magnetite → hematite.

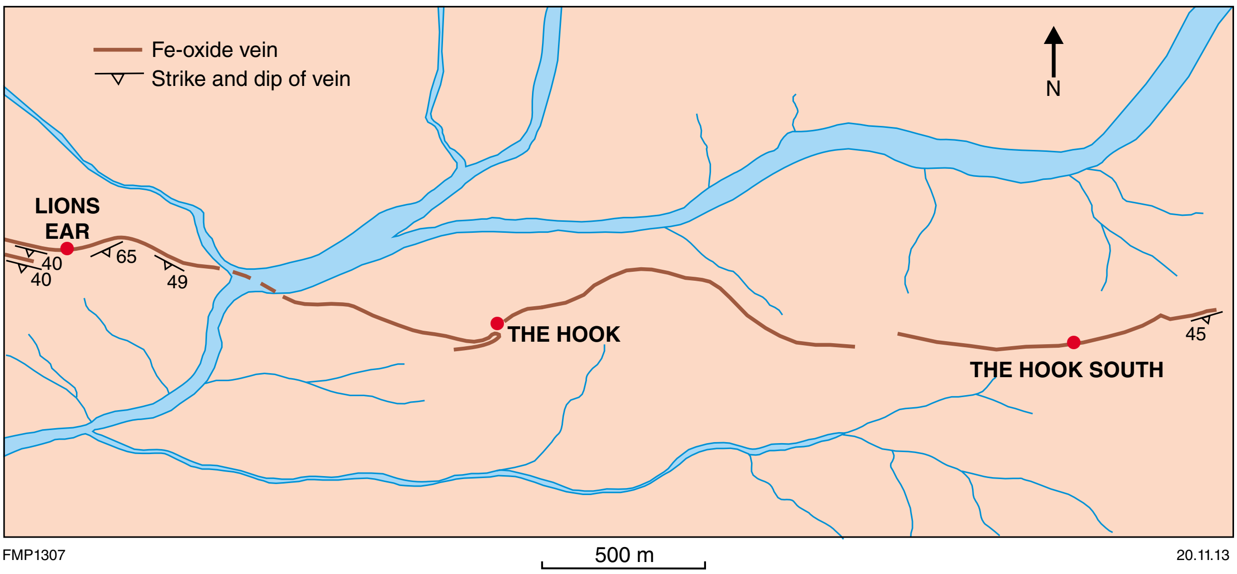

Figure 9. Ironstone veins of the Hook and Hook South prospect; after Pooley (1988) (no coordinates shown in the original report; refer to Figure 2b for approximate position)

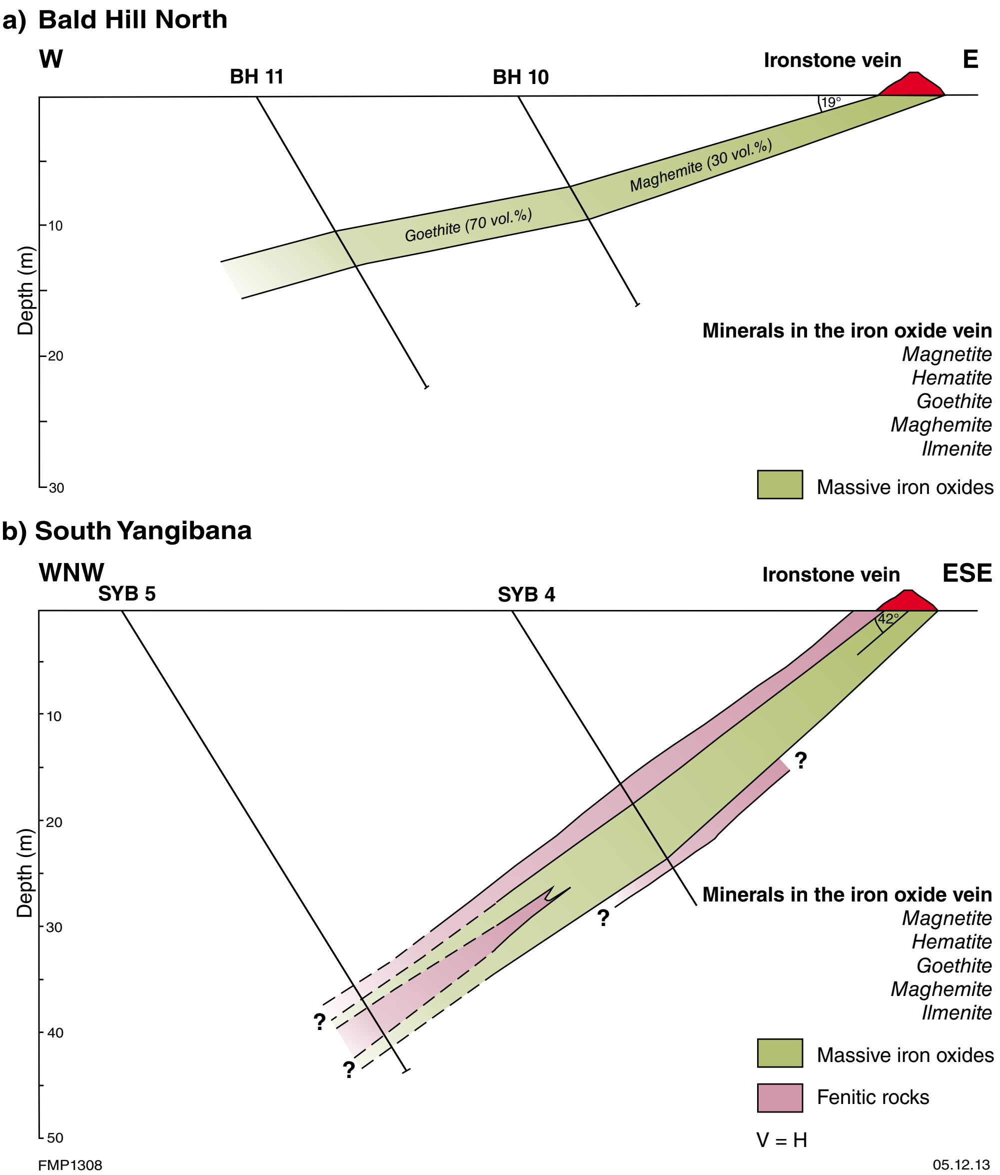

Figure 10. Cross-sectional interpretations of the Yangibana prospect, cross section interpreted from shallow RC drilling; after Pooley (1989), (no coordinates shown in the original report; refer to Figure 2b for approximate position)

Fenitic alteration haloes

Closer inspection of the GFC ironstones shows that they have narrow margins of iron-rich carbonatites associated with zones of alteration that have a distinct fenitic character. These fenitic haloes are best developed in the footwall of the ironstone veins and are characterized by the presence of orthoclase, albite, riebeckite, magnesio-arfvedsonite, aegirine and magnetite as the main mineral phases. Lesser quantities of other minerals in the fenitized rocks include cancrinite [empirical formula (ef) is $3H_2O.4Na_2O.CaO.4Al_2O_3.9SiO_2.2CO_2$] and lamprophyllite [ef is $Na_2Sr_2BaTi_3Si_4O_{14}(OH)_2F$], as well as variable amounts of nepheline and sodalite. Fenitic alteration is spatially associated with the ferrocarbonatites; however, it can also occur as discrete veins and veinlets in basement granitic rocks (Pimbyana and Yangibana Granites) (Fig. 6). In some cases monomineralic feldspar zones are present (Fig. 6b), with the rock best described as orthoclasite.

These minerals are the main components of fenitic alteration, and occur in varying amounts, presumably due to, not only the composition of the alkaline fluids, but also the primary mineralogy of the rocks affected. This results in a variety of textures and dominant mineralogy. Furthermore, petrological analysis shows that the fenitization process is highly dynamic and multiphase. For example, there are at least two generations of aegirine–augite / aegirine: coarse-grained, and very fine grained granular aggregates, overprinted by acicular riebeckite

(Fig. 11a). In addition, fine-grained aegirine also occurs as late veinlets. In the same rock isolated euhedral pyrochlore (Fig. 11b), slightly pleochroic lamprophyllite crystals and stellate aggregates of green-blue riebeckite occur. With advancing fenitization, albite and orthoclase become abundant, with acicular aegirine intergrown with magnesio-arfvedsonite. The feldspathization of the affected rocks can be pervasive, resulting in rocks that appear to be syenites (Pirajno, 2012). A good example at Gifford Creek is an outcrop of a pervasively fenitized wallrock (Fig. 12a), probably a granite of the Pimbyana or Yangibana Granites, which resembles a syenite. In the same rock, relic coarse K-feldspar crystals are overprinted by felsitic masses of adularia, associated with growths of radiating needles of sodic amphibole (arfvedsonite; Fig. 12).

Fluidal textures are common in these fenites and generally consist of bands or laminae of alternating fine-grained and closely packed aggregates of K-feldspar and plagioclase (oligoclase–albite compositions) and of pale green biotite. Euhedral magnetite crystals of a later generation are aligned along bands of biotite. The feldspar bands exhibit a granular to fluidal-like texture in places (Fig. 11c). In other cases, assemblages of euhedral nepheline, forming linear granular aggregates, occur within masses or polycrystalline aggregates of biotite, with distinct green pleochroism and abundant acicular riebeckite (Fig. 11d). Minor chalcedonic quartz or zeolite minerals fill interstitial spaces or vughs. These latter minerals are attributed to later hydrothermal, possibly meteoric, activity distinct from the fenitizing fluids.

An almost pervasively fenitized porphyritic granite (Pimbyana Granite?), consists of aggregates of nepheline and sodalite/nosean, with the latter altered to analcime and bluish-green riebeckite, associated with a curious fluidal/flow texture, where epidote overprints riebeckite. According to the International Union of Geological Sciences (IUGS) system, this rock could be a foidolite; however, this is not an igneous rock but wholesale replacement by feldspathoids of a pre-existing granitoid, in other words, a fenite. Similar fenites are recorded from the Messum Complex in Namibia, where Mathias (1956) noted rocks that were completely replaced with the introduction of K-feldspar, amphibole, aegirine–augite, sodalite and analcime. Mathias (1956) referred to these rocks as theralite and he also noted that these fenites had been 'mobilized'; hence the fluidal/flow texture, seen in these rocks.

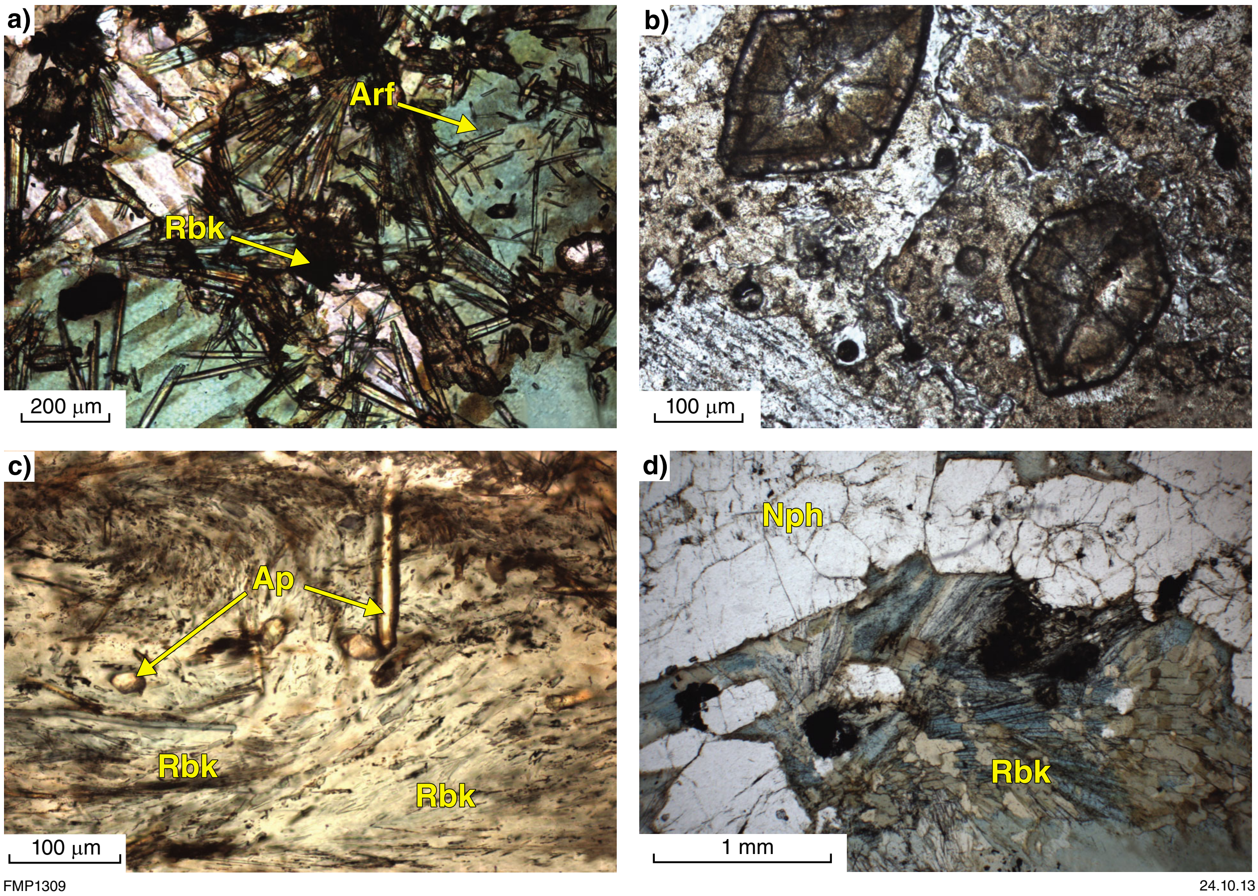

Figure 11. Photomicrographs in plane-polarized light of fenitic wallrocks at footwall of ironstone: a) GSWA 186706, acicular riebeckite (Rbk) overprinting arfvedsonite (Arf); b) GSWA 186706, zoned pyrochlore crystals; c) GSWA 186708, acicular riebeckite (Rbk) and apatite (Ap) crystals in a fluidal texture; d) GSWA 186708, nepheline (Nph) crystals and acicular riebeckite (Rbk)

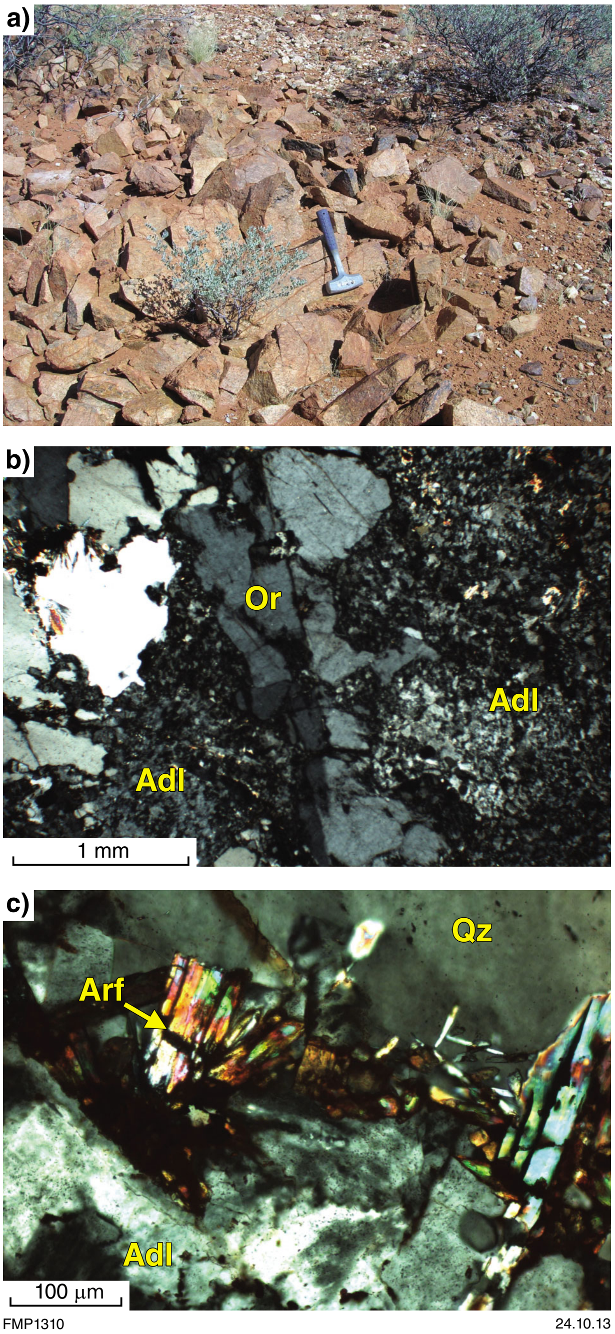

Figure 12. **a) Outcrop of fenitized granite, resembling a syenitic rock; b) GSWA 197997, photomicrographs in transmitted cross-polars showing plumose adularia (Adl) replacing orthoclase (Or) of the original granitoid; c) GSWA 197997, arfvedsonite (Arf) needles growing in the interstices between plumose adularia (Adl) and quartz (Qz)**

An outstanding illustration of a texture relating to fenitizing fluids can be seen in Figure 13a, in which a fractured and coarse-grained albite assemblage is cut by veinlets of mica phlogopite or biotite. Additionally, interstitial zones of adularia, forming a granular to felsitic aggregate, showing a peculiar plumose texture are also present (Fig. 13b,c,d). Two distinct assemblages can be discerned here:

- coarse grained albite-dominated assemblage (albitite)
- fine grained, plumose adularia–felsitic assemblage, which flows into and cuts the albitite.

The typical flow, plumose and radiating structures of the Gifford Creek fenitic rocks surrounding the ironstones, suggest a high degree of undercooling, and are inferred to result in the fine-grained mosaic that constitutes the felsitic texture (Shelley, 1993).

Discussion

A genetic model for the ironstones of the Gifford Creek Ferrocarbonatite Complex

The ironstone veins of the GFC are rare, based on their morphology and composition, and there is no known record of similar features reported. The nearest analogue, also cited by Pearson et al. (1995), are the iron-rich, low-temperature hematite–calcite–dolomite rocks, known as 'rødberg' (red rock), which occur in the Fen carbonatite in South Norway (Andersen, 1984). Rødberg refers to disseminated and massive hematite in thin irregular veins, developed along joints and grading into the primary ferrocarbonatite over distances of 2 to 3 m. The massive hematite veins were mined as iron ore. Andersen (1984) proposed that the rødberg was formed by metasomatic alteration of the ferrocarbonatite in zones of fracturing. The rødberg material is seen to replace granular ankeritic ferrocarbonatite, mostly along fractures. However, Anderson (1984) also pointed out that the rødberg was by no means the last stage in the ferrocarbonatite mineral paragenesis; in one case a ferrocarbonatite body was found to enclose round xenoliths of rødberg. Based on the fact that rødberg replaces pre-existing ferrocarbonatite along fractures, at a more advanced stage, the entire ferrocarbonatite could be replaced by rødberg. A petrogenetic model, as envisaged by Anderson (1984), as follows.

The rødberg is initiated by exsolution of hematite from the iron-bearing carbonate. At the same time, other iron-bearing phases, such as magnetite, pyrite, and ilmenite are also oxidized to hematite and locally to rutile and sulphate species. Andersen (1984) further suggested that a mobile fluid phase had to be active in order to supply oxygen to the system and remove the soluble oxidation products. The hematite enrichment was brought about by dissolution of the iron carbonate present in the ferrocarbonatite and not by external introduction of iron. Furthermore, REE-bearing minerals, such as monazite and synchysite, being largely inert and failing to oxidize, remained in the rødberg.

A somewhat similar petrogenetic model can be envisaged for the Gifford Creek ironstones, as elaborated below. Based on field and petrographic observations described previously, we suggest that fenitization occurred during and after the emplacement of the carbonatites. This was

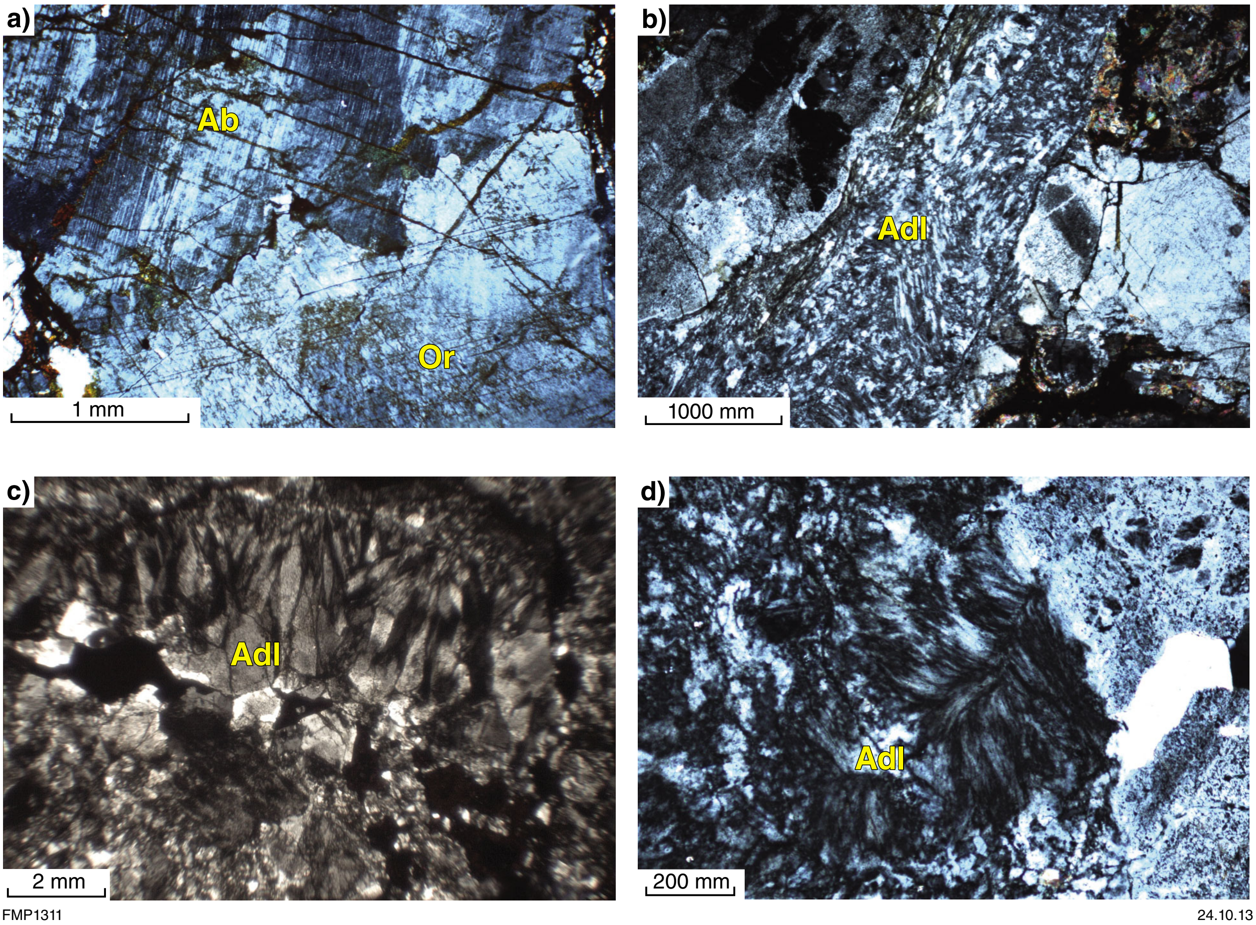

Figure 13. Transmitted light photomicrographs in crossed polars of fenitic wallrocks at footwall of an ironstone vein: a) GSWA 186724, orthoclase (Or) replacing albite (Ab); b) GSWA 186728, adularia (Adl) with rheomorphic texture, cutting and replacing albite; biotite is in the top right corner; c) GSWA 186728, adularia crystals (Adl); d) GSWA 186729, fluidal and plumose adularia (Adl)

followed by lower temperature hydrothermal activity, likely induced by the progressive cooling of carbonatite magma and the release of volatiles, during which dissolution of iron from primary magnetite, ilmenite and ferrocarbonatite minerals (dolomite, ankerite) took place. An initial stage of this high-temperature hydrothermal activity produced secondary minerals, such as biotite and phlogopite, commonly observed in the fenitic wallrocks around the ironstone veins. Some of the stages of ferruginization of the primary ferrocarbonatite and fenitic wallrocks, from early fracture-controlled to pervasive supergene replacement are shown in Figure 14. We propose a four-stage paragenetic process, which would have led to the formation of the ironstone veins, as seen today.

Stage 1 would have been characterized by the dissolution of the iron carbonates (ankerite and dolomite), and perhaps the direct conversion of igneous magnetite to form Hematite I, due to reactions, as originally proposed by Andersen (1984):

$$2\text{ ankerite} + O_2 \rightarrow Fe_2O_3 + \text{dolomite} + \text{calcite} + CO_2$$

$$2Fe_3O_4 + 0.5O_2 \rightarrow 3Fe_2O_3$$

$$2FeCO_3 + 0.5O_2 \rightarrow Fe_2O_3 + 2CO_2$$

These reactions would require higher temperatures than those usually associated with supergene processes, which are generally driven by weathering at temperatures of less than 50ºC (Taylor and Eggleton, 2001). Hematite from this stage can be seen to have developed along flow lines or laminae of the fluidal ferrocarbonatite (Fig. 14a). In stage 2, hematite is redistributed across the primary flow textures (Figs 14b.c). This is followed by the development of supergene hematite of stage 3, which overprints all previous textures (Fig. 14d). In the final stage 4, colloform hematite and goethite pervasively replace the iron oxides of the previous stages, resulting in the observed massive ironstones (Fig. 14e,f) This paragenetic sequence is illustrated in Figure 15.

Implications for the Gifford Creek Ferrocarbonatite Complex

The Gifford Creek ferrocarbonatites have a primary mineral assemblage comprising varying proportions of dolomite–ankerite, calcite, fluoroapatite and Na-amphibole. They form dyke and sill-like intrusions

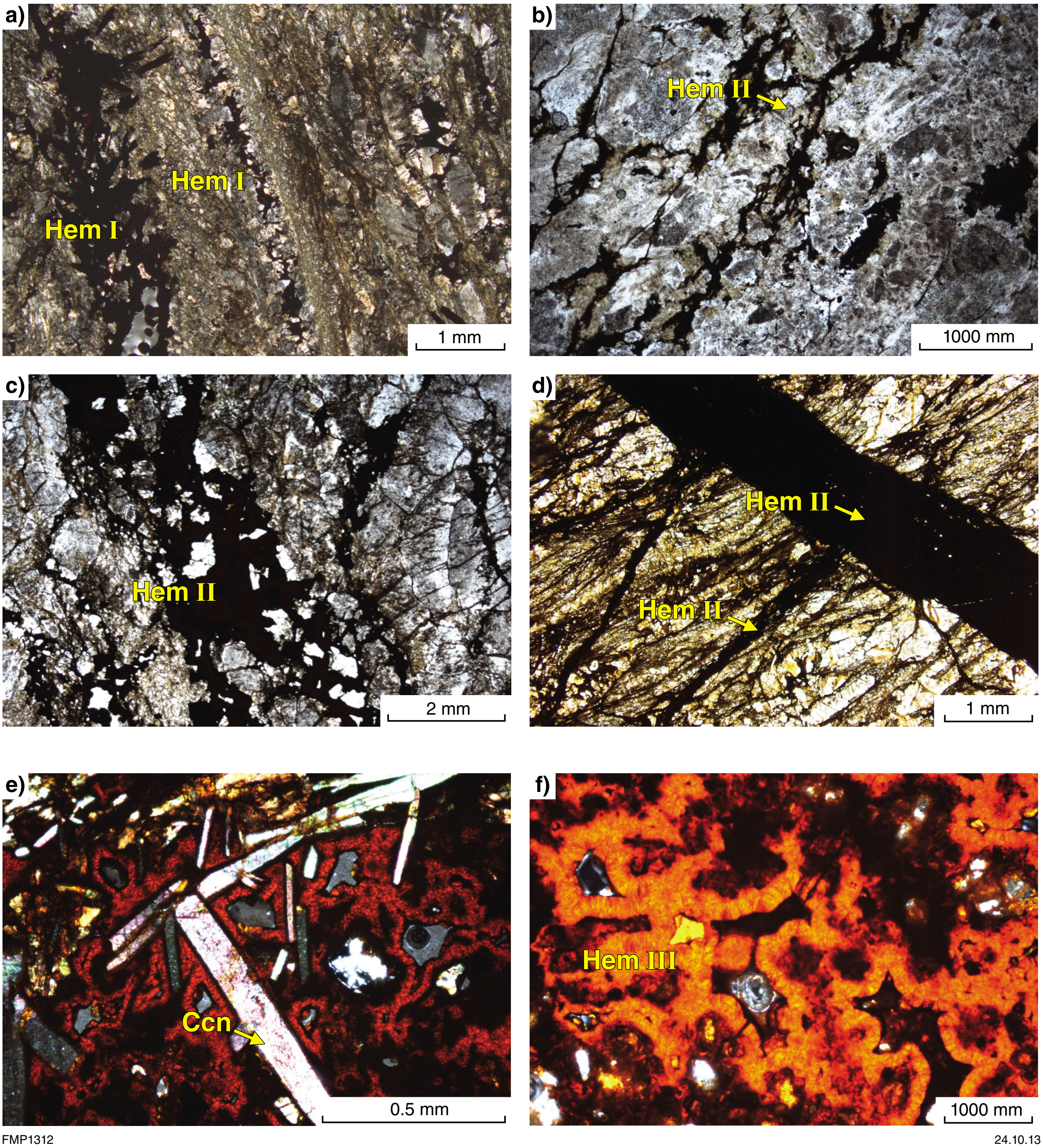

Figure 14. Photomicrographs in plane-polarized light, showing progressive replacement by iron oxides: a) GSWA 205586, hematite I (Hem I) developing along flow banding of rheomorphic fenite; b) GSWA 186728 and c) GSWA 186759, hematite II (Hem II) filling microfractures; d) GSWA 186725, hematite II cut by a hematite veinlet of a later generation (probably hematite III); e) GSWA 186759 and f) GSWA 186759, supergene colloform iron oxides, with relic cancrinite (Ccn) crystals in e)

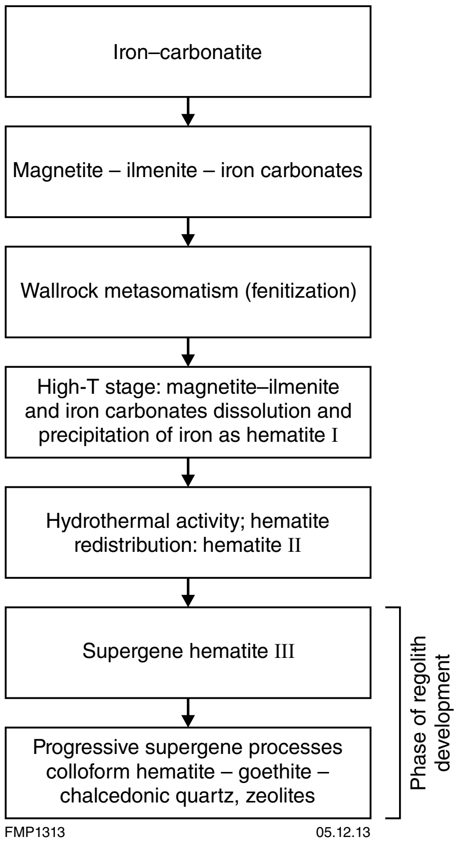

Figure 15. Flow chart (paragenetic sequence) showing a proposed model for the formation of ironstone veins in the Gifford Creek Ferrocarbonatite Complex

and are surrounded by or associated with Na–K fenitic aureoles. Fenitic rocks of the GFC are commonly rheomorphic. Fenitization is dominated by K-feldspar and albite, and varying amounts of aegirine, arfvedsonite, pyrochlore, monazite, bastnaesite and magnetite. In places, K-feldspar or albite are dominant and the rock becomes an orthoclasite or an albitite. The predominance of one or the other may be related to depth profiles. Potassic fenites (orthoclasite) tend to form around the topmost parts of a carbonatite magmatic system, whereas albitites are from deeply eroded profiles (Le Bas, 1987, 1989).

It is possible to infer the existence of a buried intrusion as a source that lies below the present level of erosion at which the ferrocarbonatite dykes and associated ironstones are exposed. Le Bas (1987) suggested that feldspathic fenites are usually linked to sövite carbonatites and are characterized by albite, co-existing with magnesio-arfvedsonite, aegirine and iron oxides. Accessory minerals in both carbonatites and fenitic haloes include fluorapatite, magnetite, phlogopite, pyrochlore, quartz, fluorite, barite, bastnaesite and monazite. All of these minerals are observed in the fenitic wallrocks, ferrocarbonatites and ferriferous derivatives of the GFC. Importantly, sövites are known to carry euhedral magnetite, co-existing with apatite, pyrochlore and micas.

Le Bas (1987) also emphasized that the ankeritic ferrocarbonatites, which sometimes replace the original sövites, tend to be of the greatest interest for economic rare metal mineralization potential. Once the carbonatite magma has consolidated, its residue is rich in volatiles (e.g. CO_2), thereby becoming a volatile-rich fluid. This is followed by progressive alteration of the primary minerals, forming calcite and the dissolution of iron-bearing minerals. This leads to replacement of the existing mineral phases, beginning along microfractures and gradually extending to form veinlets, which then coalesce into larger veins. In this somewhat simplified evolutionary scheme, it must be emphasized that fenitization and iron-dominant alteration would commonly be a complex and multiphase process. Furthermore, chemical reactions associated with fenitization and iron oxides alteration, in the case of the GFC, can totally obscure the original rock type(s).

Conclusions

The sills and dykes of ferrocarbonatites, are surrounded by large zones of fenitization (albite and K-feldspar mainly), due to wallrock interactions, accompanied by extensive fluidization due to the exsolution of abundant volatiles. The fluidized material was emplaced as arcuate and sinuous veins, which in later paragenetic stages was progressively replaced by hydrothermal iron oxides, similar to those reported by Andersen (1984) as rödberg veins and disseminations. The near surface to surface massive goethite and gossanous veins are the ending effect of supergene alteration and the development of the regolith at the GFC. Previous studies coupled with field and petrographic observations suggest that a sövite plutonic complex may underlie and may be the source of the ferrocarbonatites.

Acknowledgements

Richard Clarke carried out EDX and XRPD analyses at the Chemistry Centre (Curtin University, Perth, Western Australia). Marcus Sweetapple of CSIRO (Perth) gave an insightful and detailed review of this contribution.

References

Andersen, T 1984, Secondary processes in carbonatites: petrology of "rødberg" (hematite-calcite-dolomite carbonatite) in the Fen central complex, Telemark (South Norway): Lithos, v. 17, p. 227–245.

Flint, D and Abeysinghe, PB 2000, Geology and mineral resources of the Gascoyne Region: Geological Survey of Western Australia, Record 2000/7.

Gellatly, DC 1975, Yangibana Creek U-Th-RE-base metal prospect, Gascoyne Goldfield, WA Final Report Amax Exploration (Australia) Inc. (unpublished).

Hastings Rare Metals Limited 2012, Australian Securities Exchange (ASX) Announcement, 29 March 2012 (unpublished); <www.hastingsraremetals.com/projects/yangibana-project/previous-exploration/>.

Hoatson, DM, Jaireth, S and Miezitis Y 2011, The major rare-earth-element deposits of Australia: geological setting, exploration, and resources: Geoscience Australia, 204p.

Johnson, SP 2013, The birth of supercontinents and the Proterozoic assembly of Western Australia: Geological Survey of Western Australia, 78p.

Johnson, SP, Sheppard, S, Rasmussen B, Muhling JR, Fletcher IR, Wingate MTD, Kirkland CL and Pirajno F 2009, Meso- to Neoproterozoic reworking in the Gascoyne Complex and what it means for mineral exploration: Geological Survey of Western Australia, Record 2009/2, p. 23–25.

Johnson SP, Sheppard S,Wingate MTD, Kirkalnd CL and Belousova EA, 2011a, Temporal and hafnium iostopic evolution of the Glenburgh terrane basement: and exotic crustal fragment in the Capricorn Orogen: Geological Survey of Western Australia, Report 110, 27p.

Johnson, SP, Sheppard, S, Rasmussen, B, Wingate, MTD, Kirkland, CL, Muhling, JR, Fletcher, IR and Belousova, EA 2011b, Two collisions, two sutures: punctuated pre-1950 Ma assembly of the West Australian Craton during the Ophthalmian and Glenburgh Orogenies: Precambrian Research, v. 189, no. 3–4, p. 239–262.

Johnson, SP, Sheppard, S, Thorne, AM, Rasmussen, B, Fletcher, IR, Wingate, MTD and Cutten, HN 2011c, The role of the 1280–1250 Ma Mutherbukin Tectonic Event in shaping the crustal architecture and mineralization history of the Capricorn Orogen, *in* GSWA 2011 extended abstracts: promoting the prospectivity of Western Australia: Geological Survey of Western Australia, Record 2011/2, p. 1–3.

Le Bas, MJ 1987, Nephelinites and carbonatites, in Alkaline igneous rocks *edited by* JG Fitton and BGJ Upton: Geological Society Special Publication 30, p. 53–86.

Le Bas, MJ 1989, Diversification of carbonatites, *in* Carbonatites – Genesis and evolution *edited by* K Bell; Unwin Hyamn, London, p. 70–88.

Le Maitre, RW (editor) 2002, Igneous rocks: a classification and glossary of terms; Cambridge University Press, Cambridge, USA, 236p.

Martin, DMcB, Sheppard, S, Thorne, AM, Farrell, TR, and Groenewald, PB 2006, Proterozoic geology of the western Capricorn Orogen — a field guide: Geological Survey of Western Australia, Record 2006/18, p. 41.

Mathias, M 1956, The petrology of the Messum igneous complex, South-West Africa: Transaction of the Geological Society of South Africa, v. 59, p. 23–57.

Neuendorf, KKE, Mehl, JP and Jackson, JA 2005, Glossary of Geology, 5th edition, American Geological Institute, Alexandria,Virginia, 779p.

Newcrest Mining Ltd 1991, Gifford Creek report for the period 1/1/91 to31/12/91; Department of Mines and Petroleum, open-file report A35093, vol. I.

Pearson, JM 1996, Alkaline rocks of the Gifford Creek Complex, Gascoyne Province, Western Australia: their petrogenetic and tectonic significance; PhD thesis (unpublished); The University of Western Australia, Department of Geology and Geophysics, 286p.

Pearson, JM, Taylor, WR and Barley, ME 1996, Geology of the alkaline Gifford Creek Complex, Gascoyne Complex, Western Australia: Australian Journal of Earth Sciences, v. 43, p. 299–309.

Pearson, JM and Taylor, WR 1996, Mineralogy and geochemistry of fenitized alkaline ultrabasic sills of the Gifford Creek Complex, Gascoyne Province, Western Australia: The Canadian Mineralogist, v. 34, p. 201–219.

Pirajno, F 2012, Effects of metasomatism on mineral systems and their host rocks: alkali metasomatism, skarns, greisens, tourmalinites, rodingites, black-wall alteration and listvenites, *in* Metasomatism and metamorphism: the role of fluids in crustal and upper mantle processes *edited by* DE Harlov and H Austrheim, Lecture Series in Earth Science, Springer, p. 203–252.

Pirajno, F, Sheppard, S, Johnson, S, González-Álvarez, I, Thorne, A and Cutten, H 2010, The Gifford Creek Carbonatite Complex and Associated REE, U and Fe Oxides Mineralisation, Gascoyne Province, Western Australia: Abstracts Volume, IAGOD Symposium, Adelaide, 2010, p. 115–116.

Pooley, GD 1989, Annual Report, Reconnaissance drilling programme — indicated rare earth element potential, Gascoyne Mineral Field, Western Australia, E09/95 Annual Report; Hurlston Pty Ltd, unpublished, lodged to Department of Mines and Petroleum, Accession No. 25937; M 5479.

Shelley, D 1993, Igneous and metamorphic rocks under the microscope: Classification, textures, microstructures and mineral orientations; Chapman & Hall, London, 445p.

Sheppard, S, Rasmussen, B, Muhling, JR, Farrell, TR and Fletcher, IR 2007, Grenvillian-aged orogenesis in the Paleoproterozoic Gascoyne Complex, Western Australia: 1030–950 Ma reworking of the Proterozoic Capricorn orogeny; Journal of Metamorphic Geology, v. 25, p. 477–494.

Sheppard, S, Johnson, SP, Wingate, MTD, Kirkland, CL and Pirajno, F 2010, Explanatory notes for the Gascoyne Province: Geological Survey of Western Australia, 336p.

Sheppar,d S, Bodorkos, S, Johnson, SP, Wingate, MTD and Kirkland, CL 2011, The Paleoproterozoic Capricorn Orogeny: intracontinental reworking not continent-continent collision: Geological Survey of Western Australia, Report 108, 33p.

Taylor, G and Eggleton, RA 2001, Regolith geology and geomorphology; Wiley & Sons, Ltd, Chichester, 375p.

Wingate, MTD and Giddings, JW 2000, Age and palaeomagnetism of the Mundine Well dyke swarm, Western Australia: implications for an Australia-Laurentia connection at 755 Ma: Precambrian Research, v. 100, p. 335–357.

Wingate, MTD, Pirajno, F and Morris, PA 2004, Warakurna large igneous province: a new Mesoproterozoic large igneous province in west-central Australia; Geology, v. 32, p. 105–108.

Appendix

List of samples studied and coordinates (Zone 50)

GSWA sample no.	*Eastings*	*Northings*	*Remarks*
197986	418657	7355369	Fenite+carbonatite
197987	418657	7355369	Fenite+carbonatite
197996	414361	7351484	Iron oxides
186706	413674	7356180	Fenite
186708	425271	7353911	Fenite
186724	416921	7356860	Albite-rich fenite
186725	416921	7356860	Flow-textured fenite
186728	418577	7355252	Fenitized granite
186729	418577	7355252	Fenitized granite
186759	425474	7358655	Fenite
205586	413647	7356150	Tongue ironstone

This Record is published in digital format (PDF) and is available as a free download from the DMP website at <www.dmp.wa.gov.au/GSWApublications>.

Further details of geological products produced by the Geological Survey of Western Australia can be obtained by contacting:

Information Centre
Department of Mines and Petroleum
100 Plain Street
EAST PERTH WESTERN AUSTRALIA 6004
Phone: (08) 9222 3459 Fax: (08) 9222 3444
www.dmp.wa.gov.au/GSWApublications

RECORD 2013/12

THE IRONSTONE VEINS OF THE GIFFORD CREEK FERROCARBONATITE COMPLEX, GASCOYNE PROVINCE

PIRAJNO & GONZÁLEZ-ÁLVAREZ